

Coronary risk factors and myocardial blood flow in patients evaluated for coronary artery disease: a quantitative [^{15}O]H $_2\text{O}$ PET/CT study

Ibrahim Danad · Pieter G. Raijmakers · Yolande E. Appelman · Hendrik J. Harms · Stefan de Haan · Mijntje L. P. van den Oever · Cornelis van Kuijk · Cornelis P. Allaart · Otto S. Hoekstra · Adriaan A. Lammertsma · Mark Lubberink · Albert C. van Rossum · Paul Knaapen

Received: 17 June 2011 / Accepted: 27 September 2011 / Published online: 18 October 2011
© The Author(s) 2011. This article is published with open access at Springerlink.com

Abstract

Background There has been increasing interest in quantitative myocardial blood flow (MBF) imaging over the last years and it is expected to become a routinely used technique in clinical practice. Positron emission tomography (PET) using [^{15}O]H $_2\text{O}$ is the established gold standard for quantification of MBF in vivo. A fundamental issue when performing quantitative MBF imaging is to define the limits of MBF in a clinically suitable population. The aims of the present study were to determine the limits of MBF and to determine the relationship among coronary artery disease (CAD) risk factors, gender and MBF in a predominantly symptomatic patient cohort without significant CAD.

Methods A total of 128 patients (mean age 54 ± 10 years, 50 men) with a low to intermediate pretest likelihood of CAD were referred for noninvasive evaluation of CAD using a hybrid PET/computed tomography (PET/CT) scanner. MBF

was quantified with [^{15}O]H $_2\text{O}$ at rest and during adenosine-induced hyperaemia. Obstructive CAD was excluded in these patients by means of invasive or CT-based coronary angiography.

Results Global average baseline MBF values were 0.91 ± 0.34 and 1.09 ± 0.30 $\text{ml} \cdot \text{min}^{-1} \cdot \text{g}^{-1}$ (range 0.54–2.35 and 0.59–2.75 $\text{ml} \cdot \text{min}^{-1} \cdot \text{g}^{-1}$) in men and women, respectively ($p < 0.01$). However, no gender-dependent difference in baseline MBF was seen following correction for rate-pressure product (0.98 ± 0.45 and 1.09 ± 0.30 $\text{ml} \cdot \text{min}^{-1} \cdot \text{g}^{-1}$ in men and women, respectively; $p = 0.08$). Global average hyperaemic MBF values were 3.44 ± 1.20 $\text{ml} \cdot \text{min}^{-1} \cdot \text{g}^{-1}$ in the whole study population, and 2.90 ± 0.85 and 3.78 ± 1.27 $\text{ml} \cdot \text{min}^{-1} \cdot \text{g}^{-1}$ (range 1.52–5.22 and 1.72–8.15 $\text{ml} \cdot \text{min}^{-1} \cdot \text{g}^{-1}$) in men and women, respectively ($p < 0.001$). Multivariate analysis identified male gender, age and body mass index as having an independently negative impact on hyperaemic MBF.

Conclusion Gender, age and body mass index substantially influence reference values and should be corrected for when interpreting hyperaemic MBF values.

I. Danad · Y. E. Appelman · S. de Haan · C. P. Allaart · A. C. van Rossum · P. Knaapen (✉)
Department of Cardiology,
VU University Medical Center,
De Boelelaan 1117,
1081 HV Amsterdam, The Netherlands
e-mail: p.knaapen@vumc.nl

P. G. Raijmakers · H. J. Harms · O. S. Hoekstra · A. A. Lammertsma · M. Lubberink
Department of Nuclear Medicine & PET Research,
VU University Medical Center,
Amsterdam, The Netherlands

M. L. P. van den Oever · C. van Kuijk
Department of Radiology, VU University Medical Center,
Amsterdam, The Netherlands

Keywords Myocardial blood flow · Positron emission tomography · Non-obstructive CAD · CAD risk factors · Gender

Introduction

There has been increasing interest in quantitative myocardial perfusion imaging over the last years and it is expected to become routinely implemented in clinical practice [1–3]. Myocardial blood flow (MBF) measurements add incre-

mental value to the diagnosis and evaluation of coronary artery disease (CAD) compared with qualitative perfusion imaging techniques [1, 4, 5]. Furthermore, quantitative MBF values can be used to evaluate the effect of life-style changes and pharmacological interventions in patients with CAD risk factors and impaired MBF. Positron emission tomography (PET) is the established gold standard for quantitative MBF imaging [1, 3, 4, 6]. A number of PET tracers (e.g. $[^{13}\text{N}]\text{NH}_3$, ^{82}Rb , and $[^{15}\text{O}]\text{H}_2\text{O}$) are currently available and are well validated [7–10]. Nonetheless, the number of studies that have routinely evaluated the use of quantitative MBF values in the diagnosis of CAD are scarce [5, 11]. One of the fundamental issues when performing quantitative MBF imaging, is to define lower limits of (hyperaemic) MBF. Although databases are available with normal MBF values, these data were predominantly obtained in healthy volunteers in whom CAD had not been excluded [12–14]. Furthermore, the limits of MBF values obtained from these studies are of less clinical value, taking into consideration that these studies were performed in asymptomatic individuals without multiple risk factors for CAD, which are known to affect MBF even in the absence of epicardial atherosclerosis [15].

Therefore, the aims of this study were to determine the limits of MBF and to investigate the impact of age, gender and CAD risk factors on MBF using $[^{15}\text{O}]\text{H}_2\text{O}$ PET in a large clinical cohort of patients suspected of having and with risk factors for CAD but in whom significant CAD was excluded by invasive coronary angiography (ICA) or CT-based coronary angiography (CTCA).

Methods

Patient population

Data were obtained from a cohort of 325 patients being evaluated for CAD and therefore referred for CTCA, coronary artery calcium (CAC) scoring and PET MBF measurements using a hybrid PET/CT scanner (Gemini TF 64; Philips Healthcare, Best, The Netherlands). Patients were referred because of stable (atypical) angina or an elevated risk of CAD (presence of two or more risk factors) in the absence of symptoms. Hypertension was defined as a blood pressure $\geq 140/90$ mmHg or the use of antihypertensive medication. Hypercholesterolaemia was defined as a total cholesterol level of ≥ 5 mmol/l or treatment with cholesterol-lowering medication. Patients were classified as having diabetes if they were receiving treatment with oral hypoglycaemic drugs or insulin. A positive family history of CAD was defined as the presence of CAD in first-degree relatives younger than 55 years (men) or 65 years (women). Obstructive CAD was considered to have been ruled out

when either one of the following criteria was met: (1) absence of a luminal stenosis of more than 30% as observed on ICA or a measured fractional flow reserve (FFR) of >0.8 ; and (2) when ICA was not available, a CAC score of zero combined with a CTCA of sufficient quality to enable adequate grading of all major coronary segments which did not display a noncalcified plaque. Exclusion criteria were atrial fibrillation, cardiomyopathies, renal failure defined as glomerular filtration <45 $\text{ml}\cdot\text{min}^{-1}$, second- or third-degree atrioventricular block, symptomatic asthma, or pregnancy. A total of 128 out of the 325 evaluated patients met these criteria and were evaluated in the current study (50 men, age range 32–75 years; 78 women, age range 31–83 years). None of the patients had a documented history of CAD. Electrocardiography did not show signs of a previous myocardial infarction, and echocardiography showed a normal left ventricular function without wall motion abnormalities in all patients. CAD pretest likelihood was determined according to the Diamond and Forrester criteria [16], using cut-off values of $<13.4\%$, $>87.2\%$ and in between for low, high and intermediate pretest likelihood, respectively. Patient characteristics are shown in Table 1.

PET imaging

Patients were instructed to refrain from intake of products containing caffeine or xanthine during the 24 h before the scan. After a scout CT scan for patient positioning and 2 min after the start of intravenous adenosine infusion (140 $\mu\text{g}\cdot\text{kg}^{-1}\cdot\text{min}^{-1}$), 370 MBq of $[^{15}\text{O}]\text{H}_2\text{O}$ was injected as a 5 -ml (0.8 $\text{ml}\cdot\text{s}^{-1}$) bolus, followed immediately by a 35 -ml saline flush (2 $\text{ml}\cdot\text{s}^{-1}$). A 6-min emission scan was started simultaneously with the administration of $[^{15}\text{O}]\text{H}_2\text{O}$. This dynamic scan sequence was followed immediately by a respiration-averaged low-dose CT scan to correct for attenuation (55 mAs, rotation time 1.5 s, pitch 0.825 , collimation 16×0.625 , acquiring 20 cm in 37 s) during normal breathing [17]. Adenosine infusion was terminated after the low-dose CT scan. After an interval of 10 min to allow for decay of radioactivity and washout of adenosine, an identical PET sequence was performed during resting conditions. Images were reconstructed using the 3-D row action maximum likelihood algorithm into 22 frames (1×10 , 8×5 , 4×10 , 2×15 , 3×20 , 2×30 and 2×60 s), applying all appropriate corrections. Parametric MBF images were generated and quantitatively analysed using software developed in-house (Cardiac VUer) [18, 19]. MBF was expressed in millilitres per minute per gram of perfusable tissue and analysed on a per-segment basis according to the 17-segment model of the American Heart Association [20].

Table 1 Baseline patient characteristics according to gender

	Men (<i>n</i> =50)	Women (<i>n</i> =78)	<i>p</i> -value
Age (years, mean±SD)	52±10	55±10	0.18
Risk factors for CAD			
BMI (kg·m ⁻² , mean±SD)	27±4	27±4	0.52
Diabetes mellitus, <i>n</i> (%)	11 (22)	10 (13)	0.17
Hypertension, <i>n</i> (%)	18 (36)	33 (42)	0.48
Hypercholesterolaemia, <i>n</i> (%)	12 (24)	25 (32)	0.33
Family history of premature CAD, <i>n</i> (%)	21 (42)	39 (50)	0.38
History of smoking, <i>n</i> (%)	19 (38)	33 (42)	0.63
Medication, <i>n</i> (%)			
Statins	24 (48)	39 (50)	0.83
Beta-blockers	26 (52)	48 (62)	0.29
Aspirin	28 (56)	46 (59)	0.74
ACE inhibitors	5 (10)	13 (17)	0.21
AT-II antagonists	4 (8)	14 (18)	0.09
Calcium antagonists	9 (18)	15 (19)	0.86
Long-acting nitrates	7 (14)	8 (10)	0.52
Reason for referral, <i>n</i> (%)			
Typical angina pectoris	7 (14)	18 (23)	0.21
Atypical angina pectoris	19 (38)	37 (47)	0.29
Non-anginal chest pain	16 (32)	17 (22)	0.20
High risk, no chest discomfort	8 (16)	6 (8)	0.14
Pretest likelihood of CAD, <i>n</i> (%)			
Low	10 (20)	25 (32)	0.14
Intermediate	35 (70)	45 (58)	0.16
High	5 (10)	8 (10)	0.96

CT imaging

Patients with a stable heart rate below 65 bpm (either spontaneous or after administration of oral and/or intravenous metoprolol) underwent a CT scan for CAC scoring and/or CTCA. A standard scanning protocol was applied, with a section collimation of 64×0.625 mm, a gantry rotation time of 420 ms, a tube voltage of 120 kV, and a tube current of 800–1,000 mA (for CTCA) or 100–120 mA (for CAC scoring) depending on the patient's body size. All scans were performed with electrocardiogram-gated dose modulation to decrease the radiation dose. Calcium scoring was obtained during a single breath-hold and coronary calcification was defined as a plaque with an area of 1.03 mm² and a density ≥130 HU. The CAC score was calculated according to the method described by Agatston et al. [21]. After CAC scoring, CTCA was performed, whereby a bolus of 100 ml iodinated contrast agent was injected intravenously (5 ml·s⁻¹) followed by a flush with 50 ml 0.9% NaCl. All CT scans were analysed on a 3-D workstation (Brilliance; Philips Medical Systems, Best, The Netherlands) by an experienced radiologist and cardiologist who were blinded to the PET results. The coronary tree was

evaluated according to a 16-segment coronary artery model modified from that of the American Heart Association [22].

Invasive coronary angiography

ICA was performed according to standard clinical protocols. The coronary tree was divided according to a 16-segment coronary artery model modified from that of the American Heart Association [22]. Significant CAD was ruled out when no stenosis was present or the stenosis diameter was visually scored as ≤30% or the FFR was >0.80. The FFR was measured using a 0.014-inch sensor tipped guide wire, which was introduced through a 6F or 7F guiding catheter, calibrated and advanced into the coronary artery. Furthermore, adenosine was infused either intravenously (140 µg·kg⁻¹·min⁻¹) or into the right and left coronary artery (40 µg) to induce maximal coronary hyperaemia. The FFR was calculated as the ratio of the mean distal intracoronary pressure measured with the pressure wire to the mean arterial pressure measured with the coronary catheter [23]. A stenosis with a FFR of >0.80 was considered as a haemodynamically nonsignificant stenosis. All images were interpreted by at least two experienced interventional cardiologists.

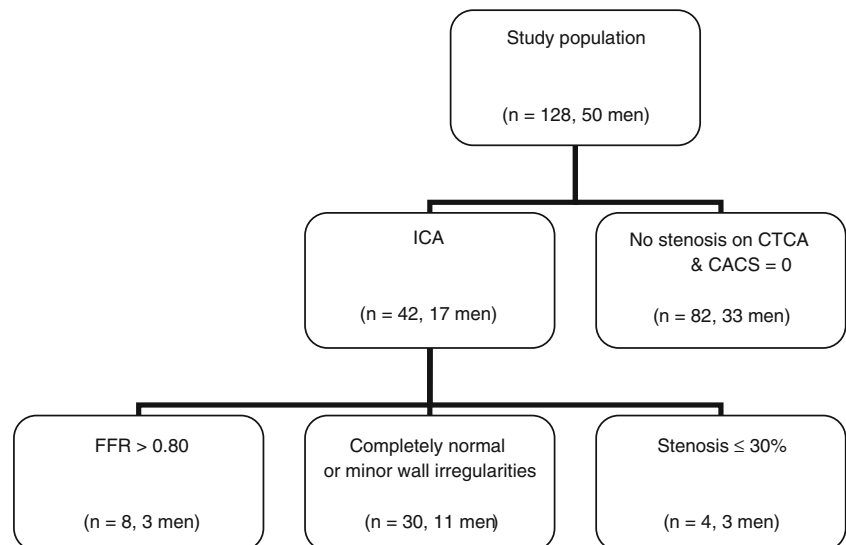
Table 2 Systemic haemodynamic characteristics of the patients at baseline and during hyperaemia

Parameter		Men (<i>n</i> =50)	Women (<i>n</i> =78)	<i>p</i> -value
Heart rate (bpm)	Baseline	60±8	62±9	0.19
	Hyperaemia	79±14	82±14	0.27
	<i>p</i> -value (overall difference)	<0.001	<0.001	
Systolic blood pressure (mmHg)	Baseline	109±16	110±16	0.65
	Hyperaemia	113±17	114±19	0.72
	<i>p</i> -value (overall difference)	0.27	0.20	
Diastolic blood pressure (mmHg)	Baseline	60±10	59±7	0.93
	Hyperaemia	60±7	59±8	0.63
	<i>p</i> -value (overall difference)	0.39	0.60	
Rate–pressure product (mmHg·min ⁻¹)	Baseline	6,523±1,423	6,876±1,551	0.20
	Hyperaemia	8,959±2,184	9,372±2,370	0.33
	<i>p</i> -value (overall difference)	<0.001	<0.001	
Mean arterial pressure (mmHg)	Baseline	76±11	76±9	0.85
	Hyperaemia	76±10	77±11	0.66
	<i>p</i> -value (overall difference)	0.90	0.64	

Data interpretation

To account for changes in baseline MBF caused by cardiac workload, baseline MBF values were corrected for the rate–pressure product (RPP), an index of myocardial oxygen consumption [24], by multiplying baseline MBF by the mean RPP in the patients as a group, divided by the RPP in the individual patient [25]. Coronary flow reserve (CFR) was defined as the ratio between hyperaemic and baseline MBF. The corrected CFR was defined as the hyperaemic MBF divided by corrected baseline MBF. Furthermore, the coefficient of variation (COV) was calculated as the ratio of the standard deviation and the mean value of the MBF multiplied by 100.

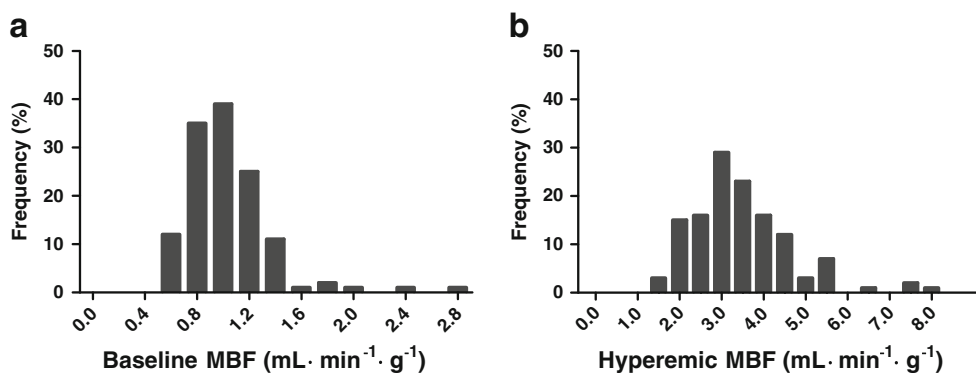
Fig. 1 Flow chart showing criteria for exclusion of obstructive CAD (ICA invasive coronary angiography, FFR fractional flow reserve, CTCA CT coronary angiography, CACS coronary artery calcium score)



Statistical analysis

Continuous variables are presented as mean values ± SD, whereas categorical variables are expressed as actual numbers. Continuous variables were compared between males and females using the paired or unpaired two-sided Student's *t*-test or the Mann-Whitney test, as appropriate. Differences between categorical variables were analysed by the chi-squared test with Yates' correction. Differences in MBF between different myocardial regions and vascular territories were compared using one-way analysis of variance with Bonferroni's correction for multiple pair-wise comparisons for localizing the source of the difference. Differences in MBF and CFR predicted by given differences in risk factors

Fig. 2 Frequency distributions of global baseline (a) and hyperaemic (b) MBF in the whole study population (a COV 31%, b COV 35%)



were estimated by linear regression analysis. Each variable was first modelled separately. All variables that were significant with univariate analyses were then entered simultaneously in a multivariate regression analyses model using backward elimination. Values of $p \leq 0.05$ were considered statistically significant. All statistical analyses were performed using SPSS software package (SPSS 15.0; Chicago, IL).

Results

Significant CAD was considered to be ruled out by ICA or CTCA (Fig. 1). As shown in Table 1, CAD risk factors and the use of medication were equally distributed between men and women. The pretest likelihood for CAD was predominantly low (27%) or intermediate (63%), and did not show a gender difference.

Haemodynamics

There was a significant increase in heart rate and RPP from baseline to hyperaemia (61 ± 9 to 81 ± 14 bpm, and 6738 ± 1506 to 9207 ± 2298 mmHg·min⁻¹, respectively; both $p < 0.001$). There were no significant changes in systolic ($p = 0.09$) or

diastolic ($p = 0.33$) blood pressure, or mean arterial pressure ($p = 0.66$). Table 2 summarizes the haemodynamic characteristics of the patients at rest and during adenosine-induced hyperaemia according to gender.

Baseline MBF

The frequency distribution of global MBF (i.e. mean flow in the whole left ventricle) is shown in Fig. 2a. MBF was 1.02 ± 0.32 ml·min⁻¹·g⁻¹ (range 0.54–2.75 ml·min⁻¹·g⁻¹, COV 31%) and the average corrected MBF was 1.05 ± 0.37 ml·min⁻¹·g⁻¹ (range 0.61–3.27 ml·min⁻¹·g⁻¹, COV 35%). Baseline MBF was significantly higher in women than in men ($p < 0.01$, Table 3). However, the corrected MBF was comparable between men and women (0.98 ± 0.45 and 1.09 ± 0.30 ml·min⁻¹·g⁻¹, range 0.61–3.27 and 0.61–2.21 ml·min⁻¹·g⁻¹, respectively; $p = 0.08$). MBF did not differ between the three vascular territories at baseline in the whole study population ($p = 0.08$). However, a significant difference was seen in baseline MBF between the anterior and inferior segments (1.12 ± 0.38 vs. 0.95 ± 0.29 ml·min⁻¹·g⁻¹; $p < 0.01$) in the whole study population and in women, owing to a diminished resting perfusion in the inferior wall (Table 3).

Table 3 Baseline MBF (ml·min⁻¹·g⁻¹) in men and women. Values are means \pm SD (range)

Parameter	Men	Women	<i>p</i> -value
Global ^a	0.91 \pm 0.34 (0.54–2.35)	1.09 \pm 0.30 (0.59–2.75)	<0.01
Vascular territory			
Left circumflex artery	0.91 \pm 0.36 (0.54–2.38)	1.12 \pm 0.30 (0.55–2.70)	<0.01
Right coronary artery	0.86 \pm 0.32 (0.40–2.33)	1.03 \pm 0.28 (0.55–2.40)	<0.01
Left anterior descending artery	0.97 \pm 0.36 (0.57–2.34)	1.11 \pm 0.34 (0.64–3.07)	0.02
<i>p</i> -value	0.33	0.16	
Myocardial region			
Septum	0.92 \pm 0.36 (0.52–2.57)	1.08 \pm 0.33 (0.58–3.02)	0.01
Inferior	0.84 \pm 0.30 (0.35–2.08)	1.01 \pm 0.27 (0.55–2.18)*	<0.01
Lateral	0.92 \pm 0.36 (0.54–2.38)	1.12 \pm 0.30 (0.55–2.70)	<0.01
Anterior	1.03 \pm 0.39 (0.56–2.45)	1.18 \pm 0.36 (0.71–3.19)	0.03
<i>p</i> -value	0.07	0.01	

* $p < 0.01$, inferior vs. anterior wall.

^aMean MBF in whole left ventricle

Table 4 Hyperaemic MBF ($\text{ml}\cdot\text{min}^{-1}\cdot\text{g}^{-1}$) in men and women. Values are means \pm SD (range)

Parameter	Men	Women	<i>p</i> -value
Global ^a	2.90 \pm 0.85 (1.52–5.22)	3.78 \pm 1.27 (1.72–8.15)	<0.001
Vascular territory			
Left circumflex artery	2.99 \pm 0.99 (1.63–6.62)	3.84 \pm 1.23 (1.74–7.89)	<0.001
Right coronary artery	2.83 \pm 0.84 (1.43–5.41)	3.67 \pm 1.34 (1.83–8.85)	<0.001
Left anterior descending artery	2.92 \pm 0.86 (1.51–5.49)	3.85 \pm 1.35 (1.60–8.38)	<0.001
<i>p</i> -value	0.67	0.61	
Myocardial region			
Septum	2.78 \pm 0.78 (1.33–4.70)	3.76 \pm 1.40 (1.71–8.67)	<0.001
Inferior	2.95 \pm 1.05 (1.39–7.00)	3.70 \pm 1.30 (1.77–8.05)	<0.01
Lateral	2.99 \pm 1.00 (1.59–6.62)	3.84 \pm 1.23 (1.74–7.89)	<0.001
Anterior	2.98 \pm 0.98 (1.38–6.31)	3.92 \pm 1.58 (1.65–9.51)	<0.001
<i>p</i> -value	0.51	0.78	

^aMean MBF in whole left ventricle

Hyperaemic MBF

The frequency distribution of global hyperaemic MBF in the whole study population is shown in Fig. 2b. MBF was $3.44\pm 1.20 \text{ ml}\cdot\text{min}^{-1}\cdot\text{g}^{-1}$ (range 1.52–8.15, COV 35%). Hyperaemic MBF was significantly higher in women than in men ($p<0.001$, Table 4). Hyperaemic MBF was distributed homogeneously throughout the myocardial walls and vascular territories in both men and women.

Coronary flow reserve

Global CFR in the whole study population was 3.57 ± 1.37 (range 1.36–9.06, COV 38%) and the average corrected CFR was 3.51 ± 1.46 (range 1.11–9.74, COV 42%). There were no differences in CFR between men and women (Table 5), and there were no differences in CFR among the three vascular territories in the whole study population ($p=0.60$). However, there was a significant difference in CFR between the anterior and inferior

segments (3.35 ± 1.41 vs. 3.86 ± 1.70 , $p=0.05$) in the whole study population. This pattern was more pronounced in men than in women (Table 5).

Impact of CAD risk factors on myocardial perfusion and flow reserve

The impact of age, gender, CAD risk factors and BMI on (hyperaemic) MBF and CFR are shown in Table 6. Except for the gender differences mentioned above, resting MBF was comparable between subgroups. Mean hyperaemic MBF was significantly lower in older patients, men and subjects with diabetes, hypercholesterolaemia and obesity (all $p<0.05$). A similar reduction in CFR was observed in these subgroups, except in obese and hypercholesterolaemic patients ($p=0.19$ and $p=0.10$, respectively). Univariate analysis showed that age ($p<0.01$), male gender ($p<0.001$), BMI ($p<0.01$) and diabetes mellitus ($p<0.01$) had a significant impact on hyperaemic MBF. In addition, multivariate analyses showed that only age, male gender and BMI independently had a negative

Table 5 CFR in men and women. Values are means \pm SD (range)

Parameter	Men	Women	<i>p</i> -value
Global ^a	3.42 \pm 1.24 (1.55–7.97)	3.67 \pm 1.45 (1.36–9.06)	0.33
Vascular territory			
Left circumflex artery	3.52 \pm 1.42 (1.64–9.88)	3.64 \pm 1.46 (1.36–9.38)	0.66
Right coronary artery	3.56 \pm 1.39 (1.44–8.93)	3.77 \pm 1.66 (1.44–10.00)	0.46
Left anterior descending artery	3.25 \pm 1.21 (1.48–7.37)	3.66 \pm 1.46 (1.26–9.36)	0.10
<i>p</i> -value	0.45	0.86	
Myocardial region			
Septum	3.27 \pm 1.17 (1.19–6.97)	3.68 \pm 1.50 (1.15–8.84)	0.10
Inferior	3.77 \pm 1.54 (1.52–10.41)	3.91 \pm 1.80 (1.62–10.33)	0.64
Lateral	3.51 \pm 1.44 (1.63–9.87)	3.64 \pm 1.46 (1.36–9.47)	0.61
Anterior	3.12 \pm 1.28 (1.23–7.36)	3.49 \pm 1.48 (1.21–9.00)	0.15
<i>p</i> -value	0.09	0.40	

^aMean CFR in whole left ventricle

Table 6 MBF and CAD risk factors. Values are means \pm SD

Factor	<i>n</i>	MBF (ml·min ⁻¹ ·g ⁻¹)		CFR
		Baseline	Hyperaemic	
Age (years)				
31–49	41	1.06 \pm 0.39	3.72 \pm 1.46	3.75 \pm 1.53
50–57	45	1.00 \pm 0.34	3.63 \pm 1.10	3.88 \pm 1.45
58–83	42	0.99 \pm 0.24	2.95 \pm 0.84*	3.07 \pm 0.93
<i>p</i> -value (overall difference)		0.58	<0.01	0.01
Gender				
Men	50	0.91 \pm 0.34	2.90 \pm 0.85	3.42 \pm 1.24
Women	78	1.09 \pm 0.30	3.78 \pm 1.27	3.67 \pm 1.45
<i>p</i> -value (<i>t</i> test)		<0.01	<0.001	0.33
Hypertension				
Yes	51	1.04 \pm 0.34	3.31 \pm 1.23	3.38 \pm 1.46
No	77	1.00 \pm 0.32	3.52 \pm 1.18	3.70 \pm 1.30
<i>p</i> -value (<i>t</i> test)		0.15	0.30	0.09
Diabetes				
Yes	21	1.03 \pm 0.45	2.70 \pm 0.61	2.80 \pm 0.72
No	107	1.02 \pm 0.30	3.58 \pm 1.23	3.73 \pm 1.42
<i>p</i> -value (<i>t</i> test)		0.67	<0.01	<0.01
History of smoking				
Yes	52	0.99 \pm 0.21	3.50 \pm 1.14	3.68 \pm 1.40
No	76	1.04 \pm 0.38	3.39 \pm 1.24	3.50 \pm 1.35
<i>p</i> -value (<i>t</i> test)		0.84	0.47	0.54
Hypercholesterolaemia				
Yes	37	1.01 \pm 0.37	3.17 \pm 1.26	3.33 \pm 1.32
No	91	1.03 \pm 0.31	3.55 \pm 1.16	3.67 \pm 1.39
<i>p</i> -value (<i>t</i> test)		0.78	0.03	0.10
Family history				
Yes	60	1.05 \pm 0.35	3.55 \pm 1.03	3.67 \pm 1.45
No	68	1.00 \pm 0.31	3.34 \pm 1.33	3.49 \pm 1.30
<i>p</i> -value (<i>t</i> test)		0.52	0.13	0.51
BMI (kg·m ⁻²)				
<25	43	1.06 \pm 0.35	3.87 \pm 1.29	3.86 \pm 1.40
25–28	42	1.01 \pm 0.38	3.37 \pm 1.12	3.55 \pm 1.19
>28	43	0.97 \pm 0.24	3.07 \pm 1.05**	3.32 \pm 1.47
<i>p</i> -value (overall difference)		0.50	<0.01	0.19

p*<0.05, age band 31–49 vs. 50–57; *p*<0.01, vs. subjects with BMI <25 kg·m⁻²

impact on hyperaemic MBF, as shown in Table 7 and Fig. 3. Univariate analysis showed that the CAD risk factors age (*p*<0.01), BMI (*p*=0.03) and diabetes mellitus (*p*<0.01) had a statistically significant negative effect on CFR. Multivariate analysis, however, showed that only age and diabetes mellitus had a negative impact on CFR, as shown in Table 7.

Discussion

In the present study in predominantly symptomatic patients who were evaluated for the presence of CAD hyperaemic

MBF was higher in women and was independently and inversely correlated with age and body mass. Baseline MBF was also significantly higher in women, which can be ascribed predominantly to a higher metabolic demand as reflected by an increased RPP.

Resting myocardial blood flow

Average baseline MBF was 1.02 \pm 0.32 ml·min⁻¹·g⁻¹ in the current patient population and ranged from roughly 0.5 to 3.0 ml·min⁻¹·g⁻¹. Of the investigated parameters, only gender was significantly associated with resting MBF. These results are in line with those of previous studies in

Table 7 Results of univariate and multivariate linear regression analysis of hyperaemic MBF and CFR

Variable	Hyperaemic MBF				CFR			
	Univariate analysis		Multivariate analysis		Univariate analysis		Multivariate analysis	
	β	<i>p</i> -value	β	<i>p</i> -value	β	<i>p</i> -value	β	<i>p</i> -value
Age	-0.03	<0.01	-0.04	<0.001	-0.03	<0.01	-0.03	0.02
Gender (male)	-0.88	<0.001	-0.94	<0.001	-0.25	0.33	-	-
BMI	-0.08	<0.01	-0.07	<0.01	-0.06	0.03	-	-
Diabetes mellitus type II	-0.88	<0.01	-	-	-0.92	<0.01	-0.80	0.01
Hypertension	-0.22	0.32	-	-	-0.32	0.20	-	-
Hypercholesterolaemia	-0.38	0.10	-	-	-0.34	0.21	-	-
Smoking history	0.11	0.61	-	-	0.18	0.47	-	-
Family history of CAD	0.20	0.34	-	-	0.18	0.47	-	-

healthy subjects, which have demonstrated higher resting MBF in women [12, 13, 26, 27]. This gender-related difference could be explained by differences in haemodynamic conditions, and were no longer apparent when MBF was corrected for the RPP. This indicates that resting MBF is autoregulated to meet metabolic demand which is dictated by heart rate, left ventricular wall stress and contractile function. Therefore, RPP can be used for indexing baseline MBF to cardiac workload. However, it should be noted that some previous studies have demonstrated that even after correction for RPP, resting MBF remains higher in women [12]. Clearly more studies are warranted to further investigate the determinants of resting MBF. Nonetheless, quantitative resting MBF is not likely to play an important role in the detection of CAD as studies have already established that epicardial CAD does not affect resting MBF until the point of subtotal obstruction [25, 28].

Resting MBF displayed regional differences where values in the inferior wall were lower than in other myocardial segments. This pattern has been observed previously in resting MBF determined using [^{15}O]H $_2\text{O}$ [12]. Although physiological heterogeneity in perfusion could be responsible, spillover artefacts from abdominal organs (e.g. liver) probably also account for these (small) differences.

Hyperaemic myocardial blood flow

Hyperaemic MBF was distributed homogeneously across the myocardium with an average of $3.44 \pm 1.20 \text{ ml} \cdot \text{min}^{-1} \cdot \text{g}^{-1}$ in the whole study population, and varied considerably among subjects ranging from approximately 1.5 to $8.0 \text{ ml} \cdot \text{min}^{-1} \cdot \text{g}^{-1}$. This wide range and homogeneous pattern of hyperaemic MBF is in agreement with previous data obtained in healthy individuals [12, 27]. There was a distinct difference between the genders with a substantial higher perfusion in women despite similar baseline

characteristics in terms of age, CAD risk profile and pretest likelihood for CAD. Multivariate analysis revealed that besides gender, age and obesity were also associated with reduced stress perfusion. These risk factors have long been recognized to induce increased coronary microvascular resistance and hence limit hyperaemic MBF [15]. It is therefore reasonable to assume that a proportion of the current population had a diminished hyperaemic MBF as a consequence of coronary microvascular disease, reflecting the functional counterpart of CAD risk factors. However, it is rather difficult to exactly identify these subjects given the large heterogeneity of perfusion values observed in the present study and in asymptomatic subjects without CAD risk factors [12]. Relative to these risk factors, however, gender exerted the biggest influence on hyperaemic MBF [13, 26]. Some hypotheses have been postulated to account for this phenomenon. First, the protective effect of oestrogen on the coronary vasculature might preserve its function in women. However, in the current study, gender-related discrepancies in hyperaemic perfusion remained when only women over 50 years were included in the analysis, which suggests that the observed difference may not be completely explained by a direct effect of oestrogen. Indeed, Duvernoy et al. showed that in postmenopausal women, hyperaemic MBF remained significantly higher than in men [26]. Furthermore, postmenopausal women receiving hormone therapy display similar hyperaemic MBF values to postmenopausal women without hormone therapy, suggesting that hormonal milieu does not significantly affect minimal microvascular resistance [29]. Second, it has been suggested that women may have a different response to adenosine, resulting in a greater catecholamine response, which may lead to an additional rise in MBF [26, 30].

Irrespective of the underlying causes that account for the differences in hyperaemic perfusion, an attempt should

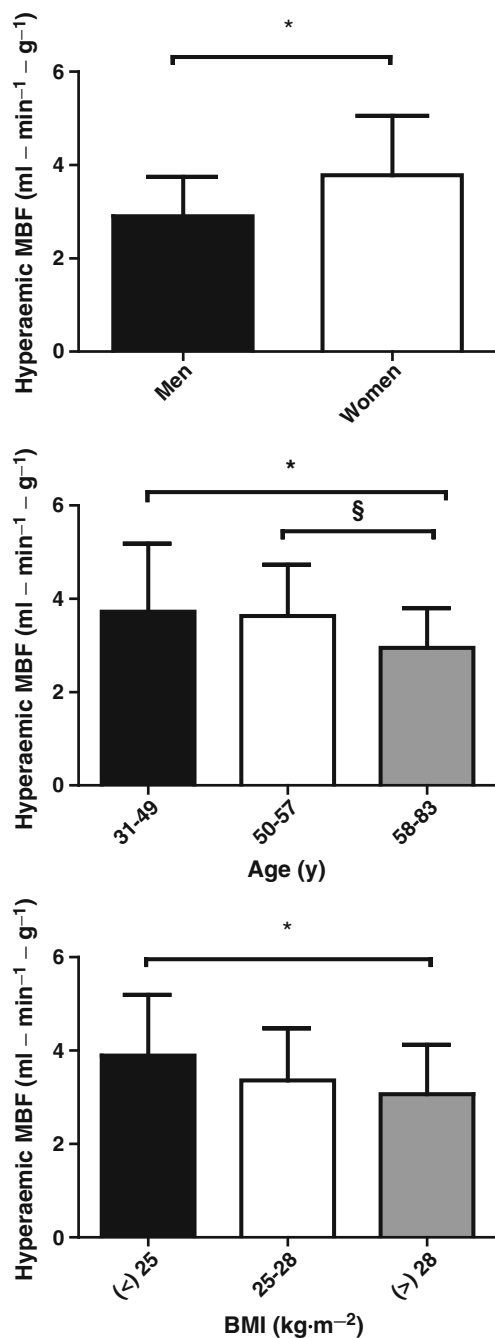


Fig. 3 Hyperaemic MBF in relation to gender, age and BMI. * $p < 0.05$

preferably be made to include gender in defining normal MBF values, although further studies are warranted to investigate gender-related differences in normal vasomotor function. Therefore, the cut-off value for detection of a flow-limiting, i.e. significant, stenosis will probably yield different values for men and women. However, given the heterogeneity of perfusion values as observed in the present study, it may prove difficult to define an optimal cut-off value for diagnostic accuracy. Of the traditional CAD risk factors, BMI had a relatively large effect upon hyperaemic

MBF. Obese patients showed a significantly reduced MBF during stress as compared to patients with a normal BMI. This is in line with the findings of Schindler et al., who found a decreased hyperaemic MBF in obese individuals without traditional CAD risk factors using [¹³N]NH₃ PET [31]. The aetiology of the link between obesity and a decreased hyperaemic MBF is not completely understood, but may very well be multifactorial, including lipid disorders, inflammation with increased oxygen radicals and insulin resistance. Regardless of the exact mechanistic link between obesity and reduced hyperaemic MBF, the current data support the opinion that obesity is a major but modifiable risk factor for the development of coronary atherosclerosis.

Coronary flow reserve

The average CFR in the present study was 3.46 ± 1.32 , and varied considerably among subjects ranging from approximately 1.2 to 9.0. Owing to the increased MBF during both resting and stress conditions in women, no gender-related differences were observed in CFR, which is consistent with previous data [26]. Given the wide range in CFR, defining normal values and optimal thresholds for identifying haemodynamically significant CAD is rather difficult. In fact, it has been shown that measurement of absolute hyperaemic MBF is superior to CFR for identifying haemodynamically significant CAD [32]. The dependency of CFR on both baseline and hyperaemic MBF probably contributes to these observations, as a reduction in CFR is not necessarily a reflection of a reduced hyperaemic MBF, but could be a result of high baseline values. Therefore, CFR for the identification of CAD is probably of less value in detecting haemodynamically significant CAD than quantitative hyperaemic MBF measurements alone. This implies that a single measurement of hyperaemic MBF could suffice in diagnostic imaging protocols. Needless to mention, more studies are needed to substantiate this hypothesis. Of interest, multivariate analysis revealed that only aging and the presence of diabetes were independently related to a diminished CFR. Cut-off values for identification of CAD using CFR therefore appear to be less influenced by gender and risk profile than to hyperaemic MBF, and would therefore potentially require less consideration of specific subgroups.

Study limitations

Some limitations of our study that may have affected the current findings must be acknowledged. First, significant CAD was presumed to have been excluded by ICA or CTCA. ICA was only performed in 42 patients, so the presence of significant CAD could not be entirely ruled out in the present study population. Although CTCA is an

excellent tool for ruling out significant CAD with a negative predictive value of 97% to 99% [33], some patients with haemodynamically significant coronary lesions may have been included. Second, subjects with obstructive CAD were not included in the current study. Therefore, more quantitative perfusion studies in a larger number of patients with and without clearly defined CAD are warranted to define the optimal diagnostic threshold for absolute MBF. Third, in the subgroup analyses the studied patient population was too small to draw definite conclusions. In contrast to other studies, hypertension, hypercholesterolaemia and diabetes mellitus appeared not to be independent predictors of a reduced hyperaemic MBF, but this might have been a result of the small study population. Furthermore, in the present study [^{15}O]H $_2\text{O}$ was used as perfusion tracer, which is not widely available. However, several studies have demonstrated that [^{13}N]NH $_3$ should provide comparable estimates of MBF over a wide range of flow velocities [34, 35]. Regarding ^{82}Rb , there are limited data available comparing ^{82}Rb with established quantitative flow tracers such as [^{13}N]NH $_3$ and [^{15}O]H $_2\text{O}$. These results suggest that MBF values obtained using ^{82}Rb would be in fair agreement with the validated flow tracers mentioned above [36, 37]. Clearly more studies seeking to quantify MBF with ^{82}Rb PET are warranted. Finally, it must be emphasized that the current data were obtained in patients without a history of cardiac disease and with normal left ventricular function. Consequently, the currently observed reference flow values cannot be applied to patients with prior coronary revascularization procedures and/or heart failure, which markedly affect MBF values in the absence of significant coronary stenoses [38–40].

Conclusion

Gender, age and BMI substantially influence reference values and should preferably be corrected for when interpreting hyperaemic MBF values.

Acknowledgments We thank Judith van Es, Robin Hemminga, Amina Elouahmani, and Nasserah Sais for performing the scans and Kevin Takkenkamp and Henri Greuter for producing the ^{15}O -labelled tracers.

Conflicts of interest None

Open Access This article is distributed under the terms of the Creative Commons Attribution Noncommercial License which permits any noncommercial use, distribution, and reproduction in any medium, provided the original author(s) and source are credited.

References

1. Knuuti J, Kajander S, Maki M, Ukkonen H. Quantification of myocardial blood flow will reform the detection of CAD. *J Nucl Cardiol.* 2009;16(4):497–506.
2. Knaapen P, de Haan S, Hoekstra OS, Halbmeijer R, Appelman YE, Groothuis JG, et al. Cardiac PET-CT: advanced hybrid imaging for the detection of coronary artery disease. *Neth Heart J.* 2010;18(2):90–8.
3. Bengel FM, Higuchi T, Javadi MS, Lautamaki R. Cardiac positron emission tomography. *J Am Coll Cardiol.* 2009;54(1):1–15.
4. Di Carli MF, Hachamovitch R. New technology for noninvasive evaluation of coronary artery disease. *Circulation.* 2007;115(11):1464–80.
5. Kajander S, Joutsiniemi E, Saraste M, Pietila M, Ukkonen H, Saraste A, et al. Cardiac positron emission tomography/computed tomography imaging accurately detects anatomically and functionally significant coronary artery disease. *Circulation.* 2010;122(6):603–13.
6. Le Guludec D, Lautamaki R, Knuuti J, Bax JJ, Bengel FM. Present and future of clinical cardiovascular PET imaging in Europe – a position statement by the European Council of Nuclear Cardiology (ECNC). *Eur J Nucl Med Mol Imaging.* 2008;35(9):1709–24.
7. Muzik O, Beanlands RS, Hutchins GD, Mangner TJ, Nguyen N, Schwaiger M. Validation of nitrogen-13-ammonia tracer kinetic model for quantification of myocardial blood flow using PET. *J Nucl Med.* 1993;34(1):83–91.
8. Bergmann SR, Herrero P, Markham J, Weinheimer CJ, Walsh MN. Noninvasive quantitation of myocardial blood flow in human subjects with oxygen-15-labeled water and positron emission tomography. *J Am Coll Cardiol.* 1989;14(3):639–52.
9. Araujo LI, Lammertsma AA, Rhodes CG, McFalls EO, Lida H, Rechavia E, et al. Noninvasive quantification of regional myocardial blood flow in coronary artery disease with oxygen-15-labeled carbon dioxide inhalation and positron emission tomography. *Circulation.* 1991;83(3):875–85.
10. Lautamaki R, George RT, Kitagawa K, Higuchi T, Merrill J, Voicu C, et al. Rubidium-82 PET-CT for quantitative assessment of myocardial blood flow: validation in a canine model of coronary artery stenosis. *Eur J Nucl Med Mol Imaging.* 2009;36(4):576–86.
11. Nandalur KR, Dwamena BA, Choudhri AF, Nandalur SR, Reddy P, Carlos RC. Diagnostic performance of positron emission tomography in the detection of coronary artery disease: a meta-analysis. *Acad Radiol.* 2008;15(4):444–51.
12. Chareonthaitawee P, Kaufmann PA, Rimoldi O, Camici PG. Heterogeneity of resting and hyperemic myocardial blood flow in healthy humans. *Cardiovasc Res.* 2001;50(1):151–61.
13. Wang L, Jerosch-Herold M, Jacobs Jr DR, Shahar E, Folsom AR. Coronary risk factors and myocardial perfusion in asymptomatic adults: the Multi-Ethnic Study of Atherosclerosis (MESA). *J Am Coll Cardiol.* 2006;47(3):565–72.
14. Sdringola S, Johnson NP, Kirkeeide RL, Cid E, Gould KL. Impact of unexpected factors on quantitative myocardial perfusion and coronary flow reserve in young, asymptomatic volunteers. *JACC Cardiovasc Imaging.* 2011;4(4):402–12.
15. Kaufmann PA, Camici PG. Myocardial blood flow measurement by PET: technical aspects and clinical applications. *J Nucl Med.* 2005;46(1):75–88.
16. Diamond GA, Forrester JS. Analysis of probability as an aid in the clinical diagnosis of coronary-artery disease. *N Engl J Med.* 1979;300(24):1350–8.
17. Lubberink M, Harms HJ, Halbmeijer R, de Haan S, Knaapen P, Lammertsma AA. Low-dose quantitative myocardial blood flow imaging using ^{15}O -water and PET without attenuation correction. *J Nucl Med.* 2010;51(4):575–80.
18. Harms HJ, Knaapen P, Raijmakers PG, Lammertsma AA, Lubberink M. Cardiac Vuer: software for semi-automatic generation of parametric myocardial blood flow images from a [^{15}O]H $_2\text{O}$ PET-CT scan. *J Nucl Med.* 2010;51(2 Suppl):477.

19. Harms HJ, Knaapen P, de Haan S, Halbmeijer R, Lammertsma AA, Lubberink M. Automatic generation of absolute myocardial blood flow images using [(15)O]H(2)O and a clinical PET/CT scanner. *Eur J Nucl Med Mol Imaging*. 2011;38(5):930–9.
20. Cerqueira MD, Weissman NJ, Dilsizian V, Jacobs AK, Kaul S, Laskey WK, et al. Standardized myocardial segmentation and nomenclature for tomographic imaging of the heart: a statement for healthcare professionals from the Cardiac Imaging Committee of the Council on Clinical Cardiology of the American Heart Association. *Circulation*. 2002;105(4):539–42.
21. Agatston AS, Janowitz WR, Hildner FJ, Zusmer NR, Viamonte Jr M, Detrano R. Quantification of coronary artery calcium using ultrafast computed tomography. *J Am Coll Cardiol*. 1990;15(4):827–32.
22. Austen WG, Edwards JE, Frye RL, Gensini GG, Gott VL, Griffith LS, et al. A reporting system on patients evaluated for coronary artery disease. Report of the Ad Hoc Committee for Grading of Coronary Artery Disease, Council on Cardiovascular Surgery, American Heart Association. *Circulation*. 1975;51(4 Suppl):5–40.
23. Pijls NH, De Bruyne B, Peels K, Van Der Voort PH, Bonnier HJ, Bartunek KJ, et al. Measurement of fractional flow reserve to assess the functional severity of coronary-artery stenoses. *N Engl J Med*. 1996;334(26):1703–8.
24. Czernin J, Muller P, Chan S, Brunken RC, Porenta G, Krivokapich J, et al. Influence of age and hemodynamics on myocardial blood flow and flow reserve. *Circulation*. 1993;88(1):62–9.
25. Uren NG, Melin JA, de Bruyne B, Wijns W, Baudhuin T, Camici PG. Relation between myocardial blood flow and the severity of coronary-artery stenosis. *N Engl J Med*. 1994;330(25):1782–8.
26. Duvernoy CS, Meyer C, Seifert-Klauss V, Dayanikli F, Matsunari I, Rattenhuber J, et al. Gender differences in myocardial blood flow dynamics: lipid profile and hemodynamic effects. *J Am Coll Cardiol*. 1999;33(2):463–70.
27. Uren NG, Camici PG, Melin JA, Bol A, de Bruyne B, Radvan J, et al. Effect of aging on myocardial perfusion reserve. *J Nucl Med*. 1995;36(11):2032–6.
28. Di Carli M, Czernin J, Hoh CK, Gerbaudo VH, Brunken RC, Huang SC, et al. Relation among stenosis severity, myocardial blood flow, and flow reserve in patients with coronary artery disease. *Circulation*. 1995;91(7):1944–51.
29. Campisi R, Nathan L, Pampaloni MH, Schoder H, Sayre JW, Chaudhuri G, et al. Noninvasive assessment of coronary micro-circulatory function in postmenopausal women and effects of short-term and long-term estrogen administration. *Circulation*. 2002;105(4):425–30.
30. Johnston DL, Hodge DO, Hopfenspirger MR, Gibbons RJ. Clinical determinants of hemodynamic and symptomatic responses in 2,000 patients during adenosine scintigraphy. *Mayo Clin Proc*. 1998;73(4):314–20.
31. Schindler TH, Cardenas J, Prior JO, Facta AD, Kreissl MC, Zhang XL, et al. Relationship between increasing body weight, insulin resistance, inflammation, adipocytokine leptin, and coronary circulatory function. *J Am Coll Cardiol*. 2006;47(6):1188–95.
32. Hajjiri MM, Leavitt MB, Zheng H, Spooner AE, Fischman AJ, Gewirtz H. Comparison of positron emission tomography measurement of adenosine-stimulated absolute myocardial blood flow versus relative myocardial tracer content for physiological assessment of coronary artery stenosis severity and location. *JACC Cardiovasc Imaging*. 2009;2(6):751–8.
33. van Werkhoven JM, Heijenbrok MW, Schuijf JD, Jukema JW, Boogers MM, van der Wall EE, et al. Diagnostic accuracy of 64-slice multislice computed tomographic coronary angiography in patients with an intermediate pretest likelihood for coronary artery disease. *Am J Cardiol*. 2010;105(3):302–5.
34. Bol A, Melin JA, Vanoverschelde JL, Baudhuin T, Vogelaers D, De Pauw M, et al. Direct comparison of [13N]ammonia and [15O] water estimates of perfusion with quantification of regional myocardial blood flow by microspheres. *Circulation*. 1993;87(2):512–25.
35. Nitzsche EU, Choi Y, Czernin J, Hoh CK, Huang SC, Schelbert HR. Noninvasive quantification of myocardial blood flow in humans. A direct comparison of the [13N]ammonia and the [15O] water techniques. *Circulation*. 1996;93(11):2000–6.
36. Yoshinaga K, Manabe O, Katoh C, Chen L, Klein R, Naya M, et al. Quantitative analysis of coronary endothelial function with generator-produced 82Rb PET: comparison with 15O-labelled water PET. *Eur J Nucl Med Mol Imaging*. 2010;37(12):2233–41.
37. El Fakhri G, Kardan A, Sitek A, Dorbala S, Abi-Hatem N, Lahoud Y, et al. Reproducibility and accuracy of quantitative myocardial blood flow assessment with (82)Rb PET: comparison with (13)N-ammonia PET. *J Nucl Med*. 2009;50(7):1062–71.
38. Knaapen P, Gotte MJ, Paulus WJ, Zwanenburg JJ, Dijkmans PA, Boellaard R, et al. Does myocardial fibrosis hinder contractile function and perfusion in idiopathic dilated cardiomyopathy? PET and MR imaging study. *Radiology*. 2006;240(2):380–8.
39. Fath-Ordoubadi F, Beatt KJ, Spyrou N, Camici PG. Efficacy of coronary angioplasty for the treatment of hibernating myocardium. *Heart*. 1999;82(2):210–6.
40. Uren NG, Crake T, Lefroy DC, de Silva R, Davies GJ, Maseri A. Reduced coronary vasodilator function in infarcted and normal myocardium after myocardial infarction. *N Engl J Med*. 1994;331(4):222–7.